The published version of the paper "L. Valentini, S. Bittolo Bon, N.M. Pugno (2016). Severe graphene nanoplatelets aggregation as building block for the preparation of negative temperature coefficient and healable silicone rubber composites. Composites Science and Technology 134 125-131." is available at: http://dx.doi.org/10.1016/j.compscitech.2016.08.005.

Severe graphene nanoplatelets aggregation as building block for the preparation of negative temperature coefficient and healable silicone rubber composites

L. Valentini,* S. Bittolo Bon

Dipartimento di Ingegneria Civile e Ambientale, Università di Perugia, UdR INSTM, Strada di Pentima 4, 05100 Terni - Italy. Tel: +39 0744 492924; E-mail: luca.valentini@unipg.it

N. M. Pugno*

Laboratory of Bio-Inspired and Graphene Nanomechanics, Department of Civil, Environmental and Mechanical Engineering, University of Trento, Trento - Italy

Center for Materials and Microsystems, Fondazione Bruno Kessler, Trento - Italy

School of Engineering and Materials Science, Queen Mary Univerisity of London, Mile End Road, London - United Kingdom. E-mail: nicola.pugno@unitn.it.

Abstract

With the request of higher performance in automotive products, sealing components and materials resisting to severe conditions, the performance requirements for silicones are becoming ever more diverse and sophisticated. In this article we prepared silicone rubber (SR)-graphene nanoplatelets (GNPs) composite via liquid mixing method; the mechanical strength of the GNPs estimated by applying a simple mixture rule suggested a severe GNPs agglomeration that was confirmed by scanning electron microscopy analysis. We observe that such SR-GNPs composite behaves as a negative temperature coefficient material, exhibiting electrical resistance decrease with temperature increase. It was also shown how the damaged SR-GNPs composite can be healed by simple thermal annealing. The healing efficiency, expressed as crack length vs. annealing temperature, has been estimated applying the principles of quantum fracture mechanics. These results could satisfy many of the demanding requirements of the silicone rubber materials used in daily life and indicate that SR-GNPs composites can act as healable and temperature sensor materials for seals, hoses and automotive sector.

Keywords: A. Nano composites. B. Mechanical properties. B. Electrical properties. B. Fracture.

Introduction

Rubber materials are commonly considered the workhorse of the industrial and automotive rubber products industries [1-3]. As a significant candidate of them, the silicone rubber (SR) offers a unique combination of chemical and mechanical properties that organic elastomers cannot match. Silicone rubber withstands high and low temperatures far better than organic rubbers. Silicone rubber can be used indefinitely at 150°C with almost no changes in its properties. It withstands use even at 200°C and some products can withstand heat of 350°C for short periods. Silicone rubbers are thus suitable as a material for rubber components used in high temperatures environments. These properties make silicone rubber the most used material for applications in extreme temperature conditions due to its good thermal stability and especially excellent elasticity [4,5]. Moreover, such soft and flexible materials have attracted attention due to their potential applications in advanced strain sensors [6-8].

Silicone rubbers are usually reinforced with carbon black, carbon nanotubes and graphene nanoplatelets to obtain improvements in thermal and electrical properties [9-11]. Compared with the traditionally used reinforcing fillers like silica, graphene nanoplatelets (GNPs) have recently attracted attention as a negative temperature coefficient material [12], exhibiting rapid electrical resistance decrease with temperature increase. Kong et al. [12] demonstrated how the electrical resistance is size dependent, decreasing with increasing the graphene thickness. These findings could suggest that agglomeration can be a viable method to produce negative temperature coefficient materials. It was also found that GNPs were similar to conventional negative temperature coefficient materials and this finding suggests the potential use of GNPs based composites for temperature sensors in rubber made automotive components.

Elastomeric applications are also susceptible to mechanical and chemical damage (e.g. scratches, cuts and punctures). Such damages result in the loss of the originally intended functions of the elastomers leading to spillage, contamination, safety hazards or just lost of performance. Such

damages are particularly problematic when the elastomers are used as seals, hoses and coatings. After the occurrence of the first cracks or surface damage, the material is especially susceptible to further damage. For this reason, seals, hoses or coatings have to be frequently checked and mended or even replaced with the subsequent cost. The development of elastomers with self-healing properties, i.e. the realization of structures able to repair mechanical damage, is an important challenge from industrial point of view for the development of polymeric materials that have much greater lifespans than currently available.

For decades, the scientific community focused the attention to developing self-healing polymeric materials to improve the safety and lifetime [13]; the storage of healing agents in the materials that are released upon damage is the most used approach. This technology generally consists in the exploitation of microcapsules [14-16] which store the healing agents into the polymer matrix. The healing agent is released from the crack to then restore it. The main drawbacks of such approach consist in the possibility to heal the material only once at the same location and the reduction of mechanical properties due to the inclusion of microcapsules in the polymer matrix that behaves as defects. Very recently it was shown that silicone-based sealants exposed to a hydrocarbon flame, can be easily healed. In this case healing did not require the delivery of additional materials [17].

Another approach can be the use of a material that contains reversible bonds that can be activated subsequent to damage. In this regard, Zheng et al. [18] have demonstrated that silicone rubber that has been cut in half can completely repair itself through heat-activated reversible bonding. They showed that the healed interface had strength comparable to the cohesive strength of the undamaged elastomer. They obtained a completely self-healed silicon rubber at 90°C for 24h. The temperature thus is a crucial parameter that can be used to heal silicone rubbers and a viable method could be the addition of thermally conductive inclusions into the polymer matrix for a better heat transfer.

Because thermal conductivity of elastomers is very low, the heat build-up is harmful to elastomers, because elastomers are susceptible to thermal degradation [19,20]. Composites with carbon-based fillers showed thermal stability, light weight, and high thermal conductivity [21,22].

These properties prompt us to believe that integrating GNPs with SR might generate a novel healable composite material, which deals self-repairing by thermal annealing and temperature activation of the electrical conductivity. Our material paves potential applications in sealing and temperature sensors of automotive components.

Experimental details

Liquid rubber (GLS-50 purchased from PROCHIMA®) was used for casting with a cold cure by poly-condensation. Before using, we add to the rubber 5% of T30 catalyst (purchased from PROCHIMA®). The complete vulcanization takes 18-20 hours at room temperature. To accelerate this process, the blend was put in a warm place (30 C°), but the reaction was too fast and did not allow the escape of air bubbles.

GNPs were purchased from Cheaptubes (bulk density 0.04gr/cm^3, thickness 8-15nm, lateral dimension about 1.5 μm). GNPs were dispersed in liquid silicone rubber (1 %wt.) through the utilization of a Dispermat (500 rpm for 1 h) to facilitate the dispersion of GNPs. Then the catalyst was added. The liquid composite was deposited onto a silicone mould and the vulcanization was obtained in 18-20 h at room temperature.

The melting behaviours of the samples were tested by differential scanning calorimeter (DSC) using a TA Q200 DSC analyser under nitrogen atmosphere. Samples were heated from -80°C to 150°C, cooled to -80°C, and heated to 150°C again. In all heating and cooling cases, the rate was set at 10°Cmin^{-1}. Thermogravimetric analysis (TGA) were performed in nitrogen with a TG/DTA

Extar 6300 at a heating rate of 10°C min^{-1}. Field emission scanning microscopy (FESEM) was used to investigate the cross section of the samples obtained by fracture in liquid nitrogen.

The electrical characterization of both neat SR and SR-GNPs composite was performed, by using a computer controlled Keithley 4200 source measure unit. The electrical current was recorded by biasing the samples at 50 V and 100 V at different temperatures.

The samples were cut into strips of ~ 100 mm × 10 mm × 2,5 mm. Before healing, a 3 mm cut was made in the middle of the sample along the strip traverse direction, and then the cut sample was healed by thermal annealing up to 250°C for 2hr. The mechanical properties were measured by a universal tensile testing machine (Lloyd Instr. LR30K) with a 250 N cell at room temperature. The extension rate was 50 mm*min^{-1} and the gauge length was 50 mm.

Results and discussion

The thermal properties of neat SR and SR-GNPs composites were investigated. Figures 1(a) and 1(b) show the TGA curves and the corresponding differential thermogravimetric (DTG) analysis curves. Figure 1(b) showed that both samples decomposed with a one-step process, which meant the GNPs did not break the network of the SR. The incorporation of the GNPS did not change the onset temperature of the composites compared to that of the neat SR. DSC analysis for the SR and the SR/GNR nanocomposites was then performed and the results were shown in figure 1(c). It was known from the literature [23] that the glass transition temperature of the SR was lower than -100°C, so the endothermic peak observed in Figure 1(c) corresponds to the melting temperature. It was found that the presence of the nanofiller did not affect the melting temperature of the neat SR matrix.

Silcone rubber has high insulation resistance of 1 TΩ*m – 100 TΩ*m, and its insulating properties are stable over a wide range of temperature as confirmed by the data reported in Figure 2(a) where no change of the electrical conductivity was detected biasing the sample with 50 V up to 250 °C.

Figure 2b shows that the electrical conductivity (electrical resistance) of the SR-GNPs composite increased (decreased) with temperature. This effect of the temperature is similar to what has been observed on the GNP resistance by Kong et al. [12] and Zhuge et al. [24]. The following equation was used to model the observed temperature dependence as a negative temperature coefficient behaviour

$$R_T=R_0\exp(B*(T_0-T)/T_0T) \quad \text{(Eq. 1)}$$

where R_T is the electrical resistance as function of temperature T, B is the material constant, and R_0 is the resistance at the reference temperature (T_0 = 298 K in our case). From the data of Figure 2b, B was determined to be 3393 K in the temperature range of 298 to 523K with the respective resistance changes from 1.42×10^{12} to 6.94×10^{9} Ω, respectively. This B value is close to that of the conventional metal oxide negative temperature coefficient materials, typically in the range of 2000 to 5000 K [25].

The obtained results thus can be explained in the following way: the high resistivity of GNPS at room temperature leads to small current flowing through the composite and therefore, the conduction is low. As the temperature increases, the resistivity of GNPs decreases; thus the current flows through the sample.

The slight decrease of the conductivity vs. time observed in Figure 2b is due to a self-heating mechanism; by decreasing the resistance, the flow of the current is higher and the sample heats by Joule effect with time. Considering that the thermal expansion coefficient of silicone rubber is 2.0–2.5 times higher than other organic rubber, such thermal expansion leads to an increase of gap between the GNP inclusions, resulting in a slight decrease in electrical conductivity.

The mechanical performance of the pristine SR and the SR-GNPs nanocomposites was then tested in terms of typical strain–stress behaviour with the curves shown in figures 3(a) and 3(b). The values of fracture strength (i.e. σ_f, the maximum of the stress-strain curves), the elongation at break (i.e. EB, the ultimate strain) and the toughness (i.e. the area underlying the stress-strain curves) are summarized in figures 3(c) and 3(d). The mechanical performance of the SR-GNPs composite had an improvement of the tensile strength while the elongation at break decreased maintaining almost the same toughness. The increasing of the tensile strength of the nanocomposites indicated that GNPs and SR had interfacial adhesions, and the GNPs deserve to transfer the tensile load when the nanocomposite was stretched.

We rationalized the test on the healed samples by Quantized Fracture Mechanics (QFM) theory [26]. For an infinite sheet with a central crack of length, 2*a*, subjected to a uniform stress σ the fracture toughness is given by $K_{IC} = \sigma_f(a=0)\,[\pi(a+q/2)]^{1/2}$ where a is the crack half-length, q the fracture quantum, and $\sigma_f(a=0)$ the material unnotched strength, with the latter that can be expressed as the combination of the strength of the SR matrix ($\sigma_{f,SR}$) and the strength of the GNPs ($\sigma_{f,GNPs}$):

$$\sigma_f(a=0) = f\,\sigma_{f,GNPs} + (1-f)\,\sigma_{f,SR} \qquad \text{(Eq. 2a)}$$

whereas according to QFM the notched and unnotched strengths are related via:

$$\sigma_f(a) = \sigma_f(a=0)\,[1+2\pi\cdot a/q]^{-1/2} \qquad \text{(Eq. 2b)}$$

where f is the volume fraction of the GNPs. From Eq. (2a) we estimate an equivalent strength of graphene nanoplatelets $\sigma_{f,GNPs}$ = 43 MPa, thus suggesting agglomeration of GNP in the current composite. Note that for good GNPs dispersion with low agglomeration in rubber composites, we recently found for $\sigma_{f,GNPs}$ a value of about 800MPa [27].

Schematically for a composite formed by a matrix and a single phase material (i. e. GNPs), the agglomeration of the single phase is defined by the number n of nano-inclusions in a single agglomeration. Assuming a Weibull distribution, the mechanical resistance of the single agglomeration, $\sigma_{f,GNPs}$, rescales, with exponent α, with its size n and the number of adjacent vacancy defects m where m is the number of missing atoms [26], as it follows:

$$\sigma_{f,GNPs} \cong \sigma_1/(n*m)^{\wedge}(1/\alpha) \quad \text{(Eq. 3)}$$

where fracture mechanics would predict α=2 for 2D inclusions and σ_1 is the strength of a single layer inclusion [28]. Measuring a thickness of about 6 μm for the single GNP inclusion (see Figure 4(a)) and assuming an average stacking layer distance of about 0.35 nm [27], we obtain a value of m~150. This value is consistent with the strength a scaling law $\sigma_{Graphene}/(m*n)^{\wedge}0.5$ of defected graphene layer where $\sigma_{Graphene}$ is the graphene strength [28].

Assuming q = 0 according to classical Linear Elastic Fracture Mechanics (LEFM) theory, the fracture toughness value calculated for both set of prepared samples is 0.0280 MPa $m^{1/2}$ for SR-GNPs and 0.0348 MPa $m^{1/2}$ for SR. According to Eq. (2b), knowing the fracture strength for undamaged and 3 mm cut sample, yields q_{SR} = 3.1 mm and $q_{SR\text{-}GNPs}$ = 0.9 mm. The effect of the thermal annealing on the crack length reduction has been reported in Figure 4 (b). The healed crack length is determined from Eqs. (1) knowing the values of the fracture quantum and the fracture strength of the sample. From this figure it is clear that the annealing up to 250 °C did not allow the repairing of the initial crack of the SR sample while the composite was almost totally healed, being about 95% the ratio between the healed crack and initial crack length. Optical images confirmed the healing of the SR-GNPs composite. From the comparison of the two images it is evident that the crack in the SR-GNPs sample almost disappeared after annealing. After the annealing, the composite showed a healing efficiency of the tensile strength that was about 87% as reported in Figure 3(d). Computed values of the healed crack length according to QFM are reported in Table 1.

Previous works indicated that the thermal conductivity enhancement achieved in GNP based silicon composites is the highest reported to date in polymer composites [10,29]. In view of previous results [30], the thermal conductivity monotonously increases as the temperature and filler loading increases. Thus in our case the observed healing mechanism is attributed to an increase of the thermal conductivity due to the severe aggregation of GNPs; this result is in contrast with the findings in previous research, in which the thermal conductivity in GNP based composites is only observed at low filler loading (<20 vol%) [31]. The high healing yield, observed only for the composite, can be explained only considering the synergic effect of the high number of inclusions in the agglomeration and the large size of single inclusions. Agglomerated GNPs, work at the macromolecular level of the matrix as a heater and transfer the required energy to the matrix activating the healing of the molecules.

4. Conclusions

In summary, novel multifunctional properties of silicone rubber composite system have been reported. GNPs addition to SR demonstrated that such composite can be healed by simple thermal annealing with high yields. Also, the composite's negative temperature coefficient behaviour suggests new potential as temperature sensors. The remarkable and variable properties of such silicones as well as their wide utilization as polymeric materials suggest that these findings will be broadly applicable.

Acknowledgements

NMP is supported by the European Research Council (ERC StG Ideas 2011 BIHSNAM n. 279985, ERC PoC 2013 KNOTOUGH n. 632277, ERC PoC 2015 SILKENE nr. 693670) and by the European Commission under the Graphene Flagship (WP "Nanocomposites", n. 604391).

References

[1] Aguilar-Bolados H, Brasero J, Lopez-Manchado MA and Yazdani-Pedram M. High performance natural rubber/thermally reduced graphite oxide nanocomposites by latex technology. Composites Part B 2014;67**:**449-454.

[2] Malas A, Pal P, Giri S, Mandal A, Das CK. Synthesis and characterizations of modified expanded graphite/emulsion styrene butadiene rubber nanocomposites: Mechanical, dynamic mechanical and morphological properties. Composites Part B 2014;58:267-274.

[3] Flaifel MH, Ahmad SH, Hassan A, Bahri S, Tarawneh MaA, Yu L-J. Thermal conductivity and dynamic mechanical analysis of NiZn ferrite nanoparticles filled thermoplastic natural rubber nanocomposite. Composites Part B 2013;52:334-339.

[4] Shang SM, Gan L, Yuen MCW. Improvement of carbon nanotubes dispersion by chitosan salt and its application in silicone rubber. Compos. Sci. Technol. 2013;86:129-134.

[5] Shang SM, Gan L, Yuen MCW, Jiang SX, Luo MN. Carbon nanotubes based high temperature vulcanized silicone rubber nanocomposite with excellent elasticity and electrical properties. Composites Part A 2014;66:135-141.

[6] Someya T, Kato Y, Sekitani T, Iba S, Noguchi Y, Murase Y, Kawaguchi H, Sakurai T. Conformable, flexible, large-area networks of pressure and thermal sensors with organic transistor active matrixes. Proc. Natl. Acad. Sci. 2005;102:12321-12325.

[7] Takei K, Takahashi T, Ho JC, Ko H, Gillies AG, Leu PW, Fearing R S, Javey A. Nanowire active-matrix circuitry for low-voltage macroscale artificial skin. Nat. Mater. 2010;9:821-826.

[8] Yousef H, Boukallel M, Althoefer K. Tactile sensing for dexterous in-hand manipulation in robotics-A review. Sens. Actuat. A 2011;167:171-187.

[9] Shang S, Gan L, Chun-wah Yuen M, Jiang S-x, Luo NM. Carbon nanotubes based high temperature vulcanized silicone rubber nanocomposite with excellent elasticity and electrical properties. Composites: Part A 2014;66:135–141.

[10] Raza MA, Westwood A, Brown A, Hondow N, Stirling C. Characterisation of graphite nanoplatelets and the physical properties of graphite nanoplatelet/silicone composites for thermal interface applications. Carbon 2011;49:4269-4279.

[11] Zhang J, Feng S, Wang X. DC current voltage characteristics of silicone rubber filled with conductive carbon black. J. of Appl. Pol. Sci. 2004;94:587–592.

[12] Kong D, Le LT, Li Y, Zunino JL, Lee W. Temperature-dependent electrical properties of graphene inkjet-printed on flexible materials. Langmuir 2012;28:13467-13472.

[13] Chen Y, Kushner AM, Williams GA, Guan Z. Multiphase design of autonomic self-healing thermoplastic elastomers. Nat. Chem. 2012;4**:**467-472.

[14] White SR, Sottos NR, Geubelle PH, Moore JS, Kessler MR, Sriram SR, Brown EN, Viswanathan S. Autonomic healing of polymer composites. Nature 2001;409:794-797.

[15] Kratz K, Narasimhan A, Tangirala R, Moon S, Revanur R, Kundu S, Kim HS, Crosby AJ, Russell TP, Emrick T, Kolmakov G and Balazs AC. Probing and repairing damaged surfaces with nanoparticle-containing microcapsules. Nat. Nanotechnol. 2012;7:87-90.

[16] Zhao Y, Zhang W, Liao LP, Wang SJ, Li WJ. Self-healing coatings containing microcapsule. Appl. Surf. Sci. 2012;258:1915-1918.

[17] Tian X, Shaw S, Lind KR, Cademartiri L. Thermal Processing of Silicones for Green, Scalable, and Healable Superhydrophobic Coatings. Adv. Mater. 2016, DOI: 10.1002/adma.201506446.

[18] Zheng P, McCarthy TJ. A surprise from 1954: siloxane equilibration is a simple, robust, and obvious polymer self-healing mechanism. J. Am. Chem. Soc. 2012;134:2024-2027.

[19] Wang Z H, Lu, Y L, Liu, J, Dang, ZM, Zhang, LQ, Wang W. Preparation of nanoalumina/EPDM composites with good performance in thermal conductivity and mechanical properties. Polym. Adv. Technol. 2011;22:2302-2310.

[20] Zhang LQ, Wu, SM, Geng, HP, Ma, XB, Leng, Q, Feng YX. China Synthetic Rubber Ind. 1998;21:207-.

[21] Causin V, Marega C, Marigo A, Ferrara G, Ferraro A. Morphological and structural characterization of polypropylene/conductive graphite nanocomposites. Eur. Polym. J. 2006;42:3153-3161.

[22] Ganguli S, Roy AK, Anderson DP. Improved thermal conductivity for chemically functionalized exfoliated graphite/epoxy composites. Carbon 2008;46:806-817.

[23] Wang YL, Hu YA, Chen L, Gong XL, Jiang WQ, Zhang PQ. Effects of rubber/magnetic particle interactions on the performance of magnetorheological elastomers. Polym. Test 2006;25:262-267.

[24] Zhuge, F, Hu, B, He, C, Zhou, X, Liu, Z, Li, R. Mechanism of nonvolatile resistive switching in graphene oxide thin films. Carbon 2011;49:3796-3802.

[25] Kang, J, Ryu, J, Han, G, Choi, J, Yoon, W, Hahn, B, Kim, J, Ahn, C, Choi, J, Park, D. $LaNiO_3$ conducting particle dispersed $NiMn_2O_4$ nanocomposite NTC thermistor thick films by aerosol deposition. J. Alloys Compd. 2012;534:70-73.

[26] Pugno NM, Ruoff RS. Quantized fracture mechanics. Philos. Mag. 2004;27:2829-2845.

[27] Valentini L, Bittolo Bon S, Lopez-Manchado MA, Verdejo R, Pappalardo L, Bolognini A, Alvino A, Borsini S, Berardo A., Pugno NM. Synergistic effect of graphene nanoplatelets and carbon black in multifunctional EPDM nanocomposites. Comp. Sci. Technol. 2016;128:123-130.

[28] Ansari R, Ajori S, Motevalli B. Mechanical properties of defective single-layered graphene sheets via molecular dynamics simulation Superlattices and Microstructures 51 (2012) 274–289.

[29] Shahil KMF, Balandin AA. Thermal properties of graphene and multilayer graphene: Applications in thermal interface materials. Solid State Comm. 2012;152:1331–1340.

[30] Huang X, Zhi C, Jiang P. Toward effective synergetic effects from graphene nanoplatelets and carbon nanotubes on thermal conductivity of ultrahigh volume fraction nanocarbon epoxy composites. J. Phys. Chem. C 2012;116:23812 – 23820.

[31] Yu AP, Ramesh P, Sun XB, Bekyarova E, Itkis ME, Haddon, RC. Enhanced thermal conductivity in a hybrid graphite nanoplatelet-carbon nanotube filler for epoxy composites. Adv. Mater. 2008;20:4740 – 4744.

Figures

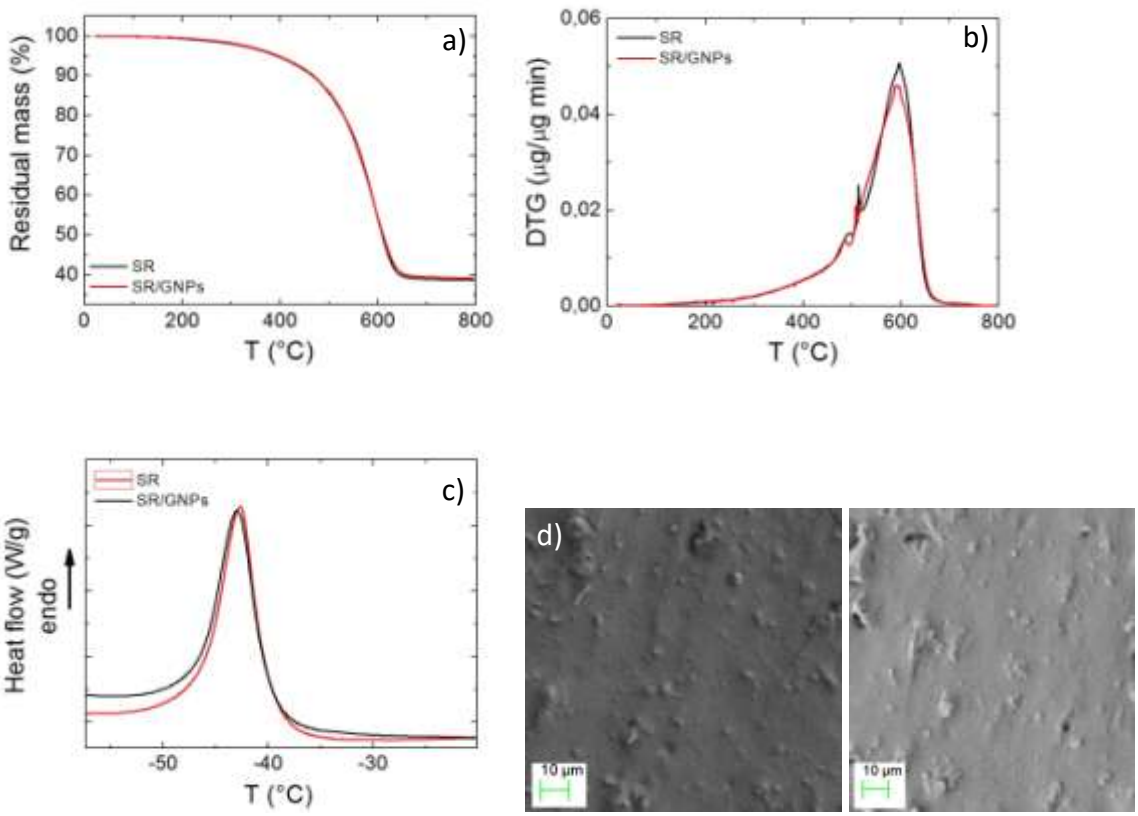

Figure 1. (a) TGA curves and corresponding (b) DTG curves of neat SR and SR-GNPs nanocomposite. (c) DSC curves of neat SR and SR-GNPs nanocomposite. (d) FESEM images of the cross sections of neat SR (left panel) and SR-GNPs nanocomposite (right panel).

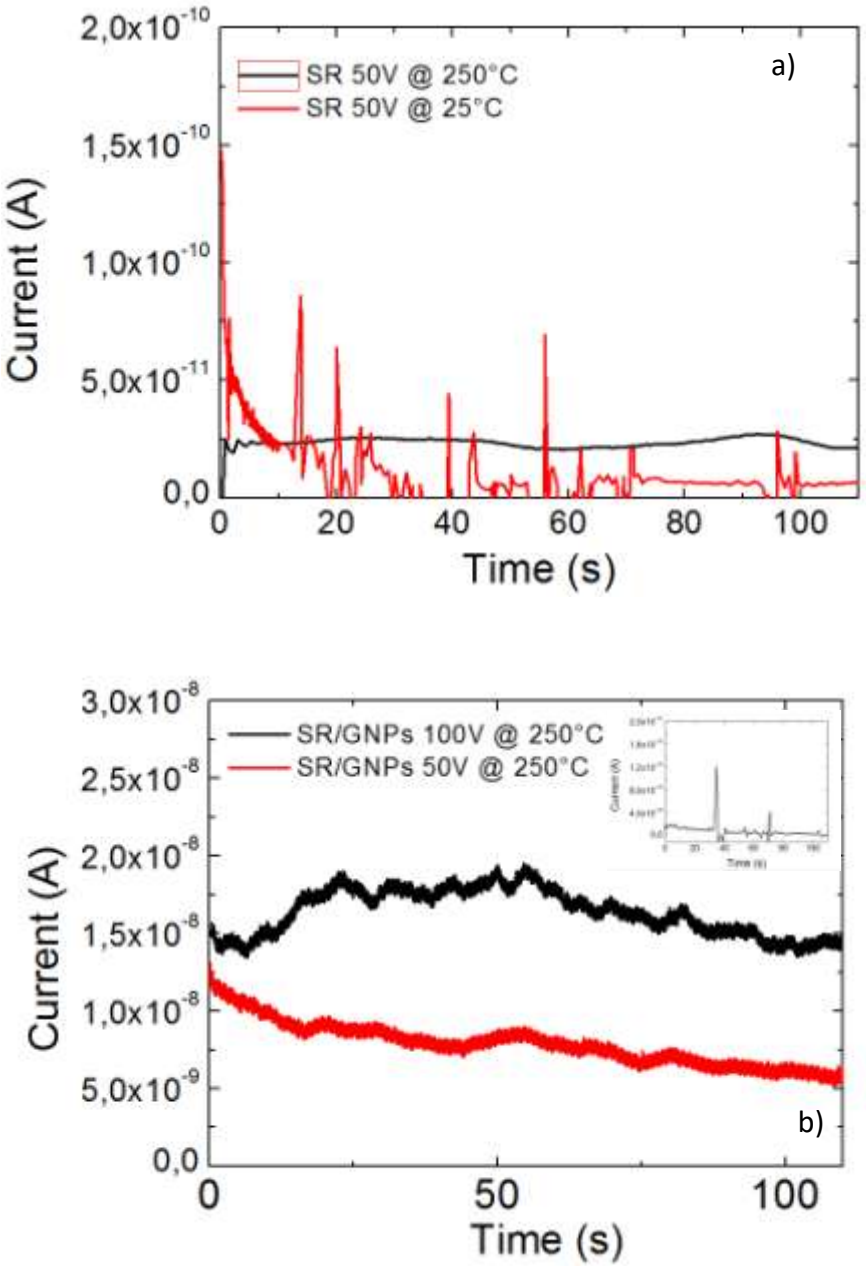

Figure 2. Current–time data of (a) SR and (b) SR-GNPs composite recorded at different bias voltages and temperatures. The inset of panel (b) shows the current-time data of SR-GNPs composite biased with 50V at room temperature.

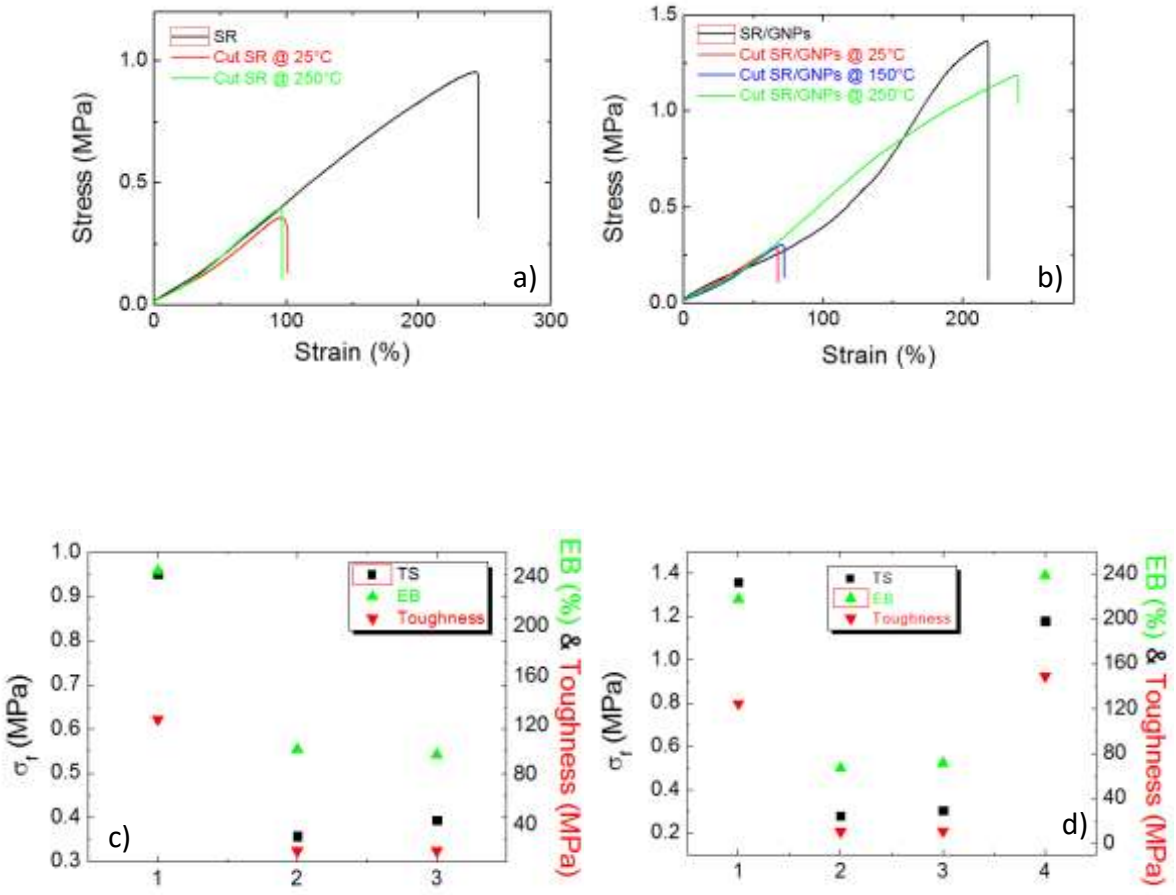

Figure 3. Stress–strain curves of (a) neat SR, cut SR and cut SR annealed at 250°C and (b) SR-GNPs composite, cut composite, cut composite annealed at 150°C and cut composite annealed at 250°C, respectively. Panel (c) shows the fracture strength, elongation at break and toughness obtained from the tensile curves of the SR (1), cut SR (2) and cut SR annealed at 250°C (3). Panel (d) shows the fracture strength, elongation at break and toughness obtained from the tensile curves of the SR-GNPs composite (1), cut SR-GNPs composite (2), cut SR-GNPs composite annealed at 150°C (3) and cut SR-GNPs composite annealed at 250°C (4), respectively.

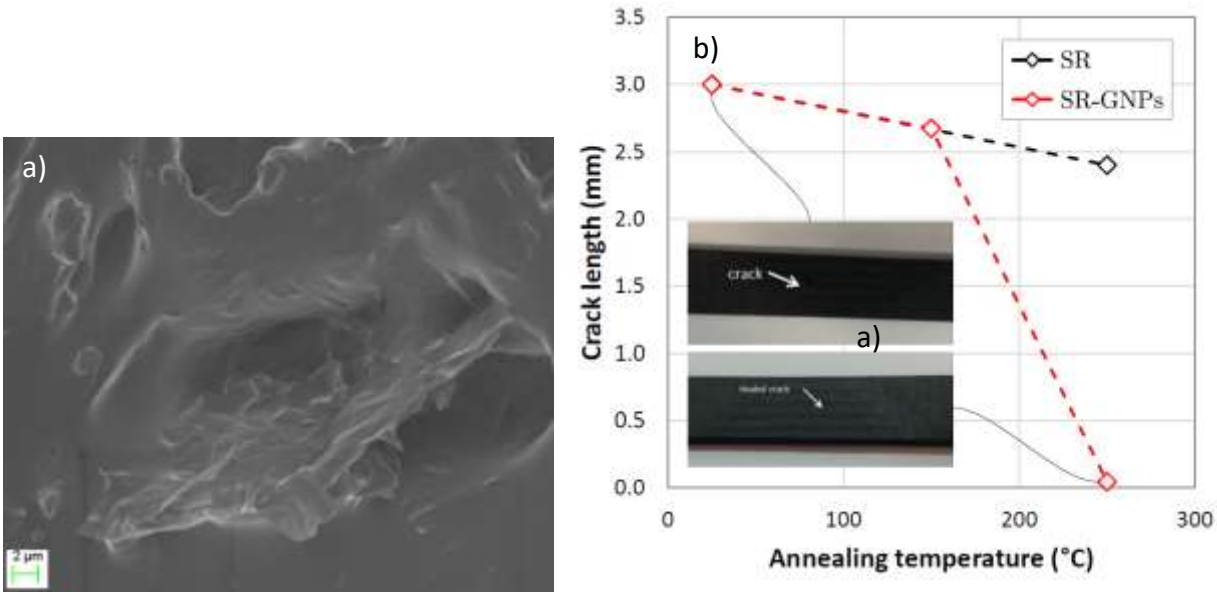

Figure 4. (a) FESEM image showing the GNP inclusion in the silicone rubber matrix. (b) Crack length vs. annealing temperature of the prepared samples from QFM estimations. The inset shows the optical images of the SR-GNPs composite before and after thermal annealing showing the healing of the initial crack length.

Table 1. Crack length vs. annealing temperature of the prepared samples from QFM estimations.

Healing temperature (°C)	**Crack length (mm)**	
	SR	**SR-GNPs**
25	3.00	3.00
150	n.a.	2.67
250	2.40	0.05